IJISET - International Journal of Innovative Science, Engineering & Technology, Vol. 3 Issue 7, July 2016
ISSN (Online) 2348 – 7968 | Impact Factor (2015) - 4.332
www.ijiset.com

Study of Physical Properties of $SrO-Fe_2O_3-V_2O_5$ oxide glasses

D. B. Sable[1], V. D. Murumkar[2] A. A. Pandit[3], K. M. Jadhav[1*]

[1] Department of Physics Dr. Babasaheb Ambedkar Marathwada University, Aurangabad, 431004 (M.S.), India
[2] Vivekanand College, Aurangabad (M.S.), India.
[3]Yashwant College Sillod, Dist. Aurangabad(M.S.), Sillod, India.

[*] drjadhavkm@gmail.com

Abstract

The oxide glass system of the composition (10-x) SrO - xFe_2O_3-90 V_2O_5, (x = 0, 2, and 4 mole %) were prepared by a standard melt quenching technique. The amorphous nature of the prepared glass was confirmed using X-ray diffraction technique (XRD). The density of prepared sample was obtained by the Archimedes principle. The physical parameters of the glasses were also determined with respect to the composition. Density increases from 3.10 to 3.15 gm/cm^3, whereas the molar volume decreases with the increase in Fe_2O_3 concentration and also to study the physical parameters like Oxygen packing density, specific volume. In order to study optical properties, absorption spectra were measured at room temperature, Energy band gap, Refractive index, Dielectric constant, Reflection loss; Molar refractivity, Molar polarizability, Metallization and Electronic polarizability are studied. Oxygen packing density is increasing with increasing the concentration of Fe_2O_3. Molar polarizability, Molar refractivity, Electronic polarizability were decreasing with increasing mole % of Fe_2O_3 respectively.

Keywords: *XRD, Physical properties.*

1. Introduction

The oxide glasses doped with the transition metal oxides such as CuO, Fe_2O_3, MO_3, WO_3, V_2O_5 etc. are of great interest because of their technological applications such as sensors in magneto-resistance effect optical switching and memory devices, cathode materials in batteries, electrical and switching device etc. [1-3].

The glasses containing transition metal oxides exhibit the semiconducting properties; semiconducting nature of V_2O_5 is due to two valence states V^{5+} and V^{4+} of vanadium [4].

Sanjay et al [5] studied the physical properties of Fe_2O_3 added $PbO-B_2O_3$ oxide glass system. Rajesh Parmar et al [6] observed that the band gap energy decreases with an increase in iron concentration, and refractive index increases with the increase in the Fe_2O_3 content in $SiO_2-Bi_2O_3-Fe_2O_3$ glass system. Safey aibrahim et al [7] observed increased density of the glass samples with the increase of the Fe_2O_3 content and that causes a corresponding decrease in the molar volume.

In the present work, physical properties such as Dielectric constant, Refractive index, Molar refractivity, Molar polarizability; Metallization, Electronic polarizability, Molar refractivity, Molar polarizability, Polarizability per unit volume etc of $SrO-Fe_2O_3-V_2O_5$ oxide glass system are presented.

2. Experimental

2.1 Sample preparation

The glass samples having a composition (10-x)SrO - $x.Fe_2O_3$- 90 V_2O_5, where, x = 0, 2, and 4 mole percentage was prepared by a melt quenching technique. Appropriate amount of analytical grade reagent as strontium carbonate ($SrCO_3$), vanadium pentoxide (V_2O_5) and ferric oxide (Fe_2O_3) were used as starting materials. The compositions used during the synthesis are tabulated in the table 1. According to stoichiometric proportion reagents were mixed together and ground for half an hour in order to have the homogeneous mixing. Then it was poured into alumina crucible and kept in muffle furnace 950°C for 1h, until a bubble-free liquid was formed. The melts were quickly cooled at room temperature by pouring and pressing between two stainless steel plates. The as prepared glass samples were powdered for further characterization.

2.2 Characterizations

X-ray diffraction (XRD) patterns of the synthesized glass samples were recorded by using Philips (Model pw-3710) X-ray diffractometer. The XRD patterns recorded at room temperature. The density of the glasses was determined at room temperature using the Archimedes principle with acetone as an immersion liquid and the molar volume also calculated from the density data. The optical absorption spectra for these glasses were recorded using UV-Perkin Elmer absorption spectrophotometer in the wavelength range 300–800 nm at normal incidence.

3. Results and discussion

The amorphous nature of the prepared samples was confirmed by from XRD studies. XRD patterns of the glasses are shown in Fig. 1, the characteristic of amorphous phase can be observed in the 2θ = 20–40˚range. The spectra did not show any sharp peaks and confirms that the glass samples are amorphous in nature.

The densities of the prepared glasses were measured at room temperature using the Archimedes displacement method in which acetone was used as immersing liquid. The density was calculated according to the formula [8, 9].

$$d_B = \frac{W_A}{W_A - W_B} \times d_{ace} \quad (1)$$

Where, W_A = in weight of the sample in air, W_B is weight of sample in acetone and d_{ace} (ρ = 0.791 gm/cm^3) is the density of acetone. Density is a powerful tool capable of exploring the changes in the structure of glasses. The addition of any transition metal ions to the glass leads to a linear variation, i.e. either increase or decrease in the density with changing compositions [10]. The values of bulk densities are given in table 2 and it can be observed that the density linearly increases from 3.10 to 3.15 gm/cm^3 with the increase in Fe_2O_3 concentration in the glass composition as shown in Fig.2.

The corresponding molar volumes were calculated by using eq. [11].

$$V_m = \frac{M}{\rho} \quad (2)$$

Here, Vm is molar volume; ρ is the density of the sample and M are the molecular weight of the sample. The molar volume values are shown in table 2.

The comparative study of the density and molar volume are exactly opposite to each other. The Variation of the density and molar volume as a function Fe_2O_3 composition (x) is shown in Fig. 2. It was observed that the density increases and the molar volume decrease with the increase in Fe_2O_3 content.

The specific volume *Vs* of a sample was then calculated as the inverse of the obtained density value. The specific volume values were decreased from 0.322 to 0.317 cm^3 .With the increases of Fe_2O_3 content as shown in table 2 [12].

The oxygen packing density of the glass samples was calculated using the following relation [13]

$$O.P.D = n\frac{M}{\rho} \quad (3)$$

The oxygen packing density is an important parameter in explaining the structure of glass.

The oxygen packing densities are increasing with the increase in Fe_2O_3 concentration in the glass composition as shown in shown in table 2.

Ultraviolet-visible spectra (UV-VIS)

Optical absorption spectra of (10-x)SrO - x.Fe_2O_3- 90 V_2O_5, where, x = 0, 2, and 4 mole glasses recorded at room temperature in the wavelength region 300–800 nm is shown in Fig. 3.(a and b).

The energy band gap of the transition metal oxide glass could be evaluated from the absorption coefficient, a near the edge of absorption curve. The absorption coefficient, a was determined by using the following relation [14, 15]

$$\alpha = 2.303\frac{A}{d} \quad (4)$$

where, A is the absorbance and d is the thickness of the samples. These transitions occur in both crystalline and amorphous semiconductor materials. These transitions are related Motts and Devi's relation [16]. For photon energies just above fundamental edge, the relation between absorption coefficient (α) and photon energy is given below [17];

$$\alpha = B\frac{(h\nu - E_g)^n}{h\nu} \quad (5)$$

where, B is a constant related to the extent of the band tailing, $h\nu$ is the photon energy, E_g is the optical energy band gap and the exponent n = ½ for an allowed direct transition, while n = 2 for an allowed in direct transition.

The Tauc plots were plotted for various values of n, that is, 1/2 and 2, corresponding to direct allowed and indirectly allowed. The plots the grapes variation of $(\alpha h\nu)^{1/2}$ vs. with hν (Tauc's plot) is shown in Fig. 4(a and b). To estimate the values of *E*g, the linear region of the curves is extrapolated to meet the *hν* axis at $(\alpha h\nu)^{1/2}$ = 0 and are shown Fig. 4(a and b).

The values of refractive index for various compositions have been determined from the optical energy band gap using the relation proposed by Dimitrov and Sakka [18].

$$\frac{n^2-1}{n^2+2} = 1 - \sqrt{\frac{E_g}{20}} \quad (6)$$

The Variation of refractive index and optical energy band gap as a function Fe_2O_3 composition (x) is shown in Fig. 5. It was observed that the refractive index decreases and the optical band gaps increase with the increase in Fe_2O_3 content. The optical dielectric constant (ε) was calculated from the refractive index of the glass using given equation [19].

$$\varepsilon = n^2 \quad (7)$$

Fig.7. It is observed that the optical dielectric constant decreases with the increase in Fe_2O_3 content.

The reflection loss (R) from the glass surface was compared from the refractive index by using the Fresnel's formula as [20]

$$R = (n-1|n+1)^2 \quad (8)$$

The reflection loss values were decreased from 0.166 to 0.150 with the increases of Fe_2O_3 concentration as shown in table 3.

The Lorentz-Lorenz equation [21] relates molar refraction Rm to refractive index n and molar volume Vm of the substance by,

$$Rm = (n^2 - 1|n^2 + 2) \times Vm \qquad (9)$$

Where, Vm is the equal to the molar volume. The molar refraction Rm values were linearly decreases from 35.02 to 32.93 cm^3 with the increases of Fe_2O_3 content as shown in table 3.

The Variation of molar refractivity Rm as a function Fe_2O_3 composition (x) is shown in Fig. 8. It was observed that the molar refraction decreases with the increase in Fe_2O_3 content. This equation gives the average molar refraction of isotropic substances, i.e., for liquids, glasses and cubic crystals. The Lorentz-Lorenz equation presents the polarizability, i.e., the magnitude of the response of the electrons to an electromagnetic field [22].

The ratio of $\frac{Rm}{Vm}$ is called polarizability per unit volume. According to the Herzfeld theory of metallization [23], If $\frac{Rm}{Vm} > 1$ and $\frac{Rm}{Vm} < 1$ predicting metallic or insulating. From Table 3 it is clear that present glass samples behave as non-metal. The difference M = 1 – Rm/Vm is the so-called metallization criterion. The metallization values were increased from 0.39 to 0.41 with the increases of Fe_2O_3 concentration as shown in table 3. Materials with large M close to 1 are typical insulators. The small value of M close to zero means that the width of both valence and conduction bands become large, resulting in a narrow band gap and increased the metallicity of the solid.

The behavior of optical dielectric constant and metallization are exactly opposite to each other. The Variation of dielectric constant and metallization as a function Fe_2O_3 composition (x) is shown in Fig. 7. It was observed that the optical dielectric constant decreases and the metallization increase with the increase in Fe_2O_3 content.

The molar refraction also shows a consistent decrease and is found to depend on the refractive index, density and average molecular weight of glass and is consistent with all the physical parameters determined. The values of reflection loss and molar refraction are listed in Table 3. Electronic polarizability of an ion is related to properties of the material such as refraction, optical nonlinearity along with optical basicity and is of significant interest to study the polarization state of ions in crystalline and amorphous materials [24, 25]. Molar refraction is related to the structure of the glass and it is proportional to the molar electronic polarizability of the material, through the Clausins– Mossotti relation [26].

$$\propto m = \frac{3Rm}{4\pi N} \qquad (10)$$

Where N is the number of polarizable ions per mole and is assumed to be equal to the Avogadro"s number (N). The value 4π/3 is known as a constant in Lorentz function. With αm in ($10^{-24}cm^3$), [27] can be transformed to Rm = 2.52 αm.

The electron polarizability αe can be calculated using the relation [28].

$$\propto e = \frac{3(n^2 - 1)}{4\pi N(n^2 + 2)} \qquad (11)$$

Molar polarizability and electronic polarizability values were decreased with the increases of Fe_2O_3 concentration as shown in table 3. Fig.9. It was observed that the Molar polarizability decreases with the increase in Fe_2O_3 content and also Fig.6.electronic polarizability decreases with the increase in Fe_2O_3 content. The behavior of the density and electronic polarizability are exactly opposite to each other. The Variation of the density and electronic polarizability as a function Fe_2O_3 composition (x) is shown in Fig. 6. It was observed that the density decreases and the electronic polarizability increase with the increase in Fe_2O_3 content.

Table 1: Coding for the samples and composition (mol %)

Sample code	Composition (mol %)		
	SrO	Fe_2O_3	V_2O_5
SFV1	10	0	90
SFV2	08	2	90
SFV3	06	4	90

SFV: Strontium oxide, Ferric-oxide, Vanadium pentoxide.

Table 2: Physical parameter: density (d), molecular weight (M), molar volume (V_m), Oxygen packing density (O), specific volume *Vs*

Sample code	d (g/cm^3)	M (g/mol)	V_m (cm^3/mol)	O (10^{-6} m^3/mole)	Vs (cm^3/mol)
SFV1	3.10	178.45	57.55	53.87	0.322
SFV2	3.12	178.69	57.23	54.55	0.320
SFV3	3.15	178.93	56.72	55.60	0.317

Table 3: Reflection loss (R), Molar refractivity (Rm), Electronic polarizability (α_e), Metallization (M), Molar polarizability (α_m) and Polarizability per unit volume (Rm/V_m)

Sample code	R	Rm (cm3)	α_e (10^{24}ions /cm3)	M	α_m (10^{24}ions /cm3)	Rm/ V_m
SFV1	0.166	35.02	0.241	0.39	1.389	0.60
SFV2	0.159	34.12	0.236	0.40	1.353	0.59
SFV3	0.150	32.93	0.230	0.41	1.306	0.58

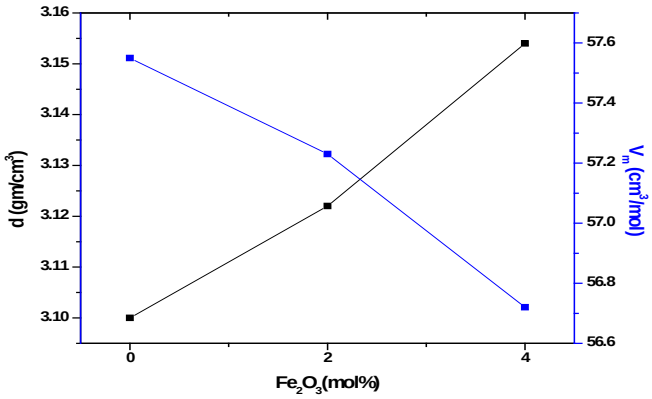

Figure 2 . Variation of density (d) and molar volume (V_m) with Fe_2O_3 content

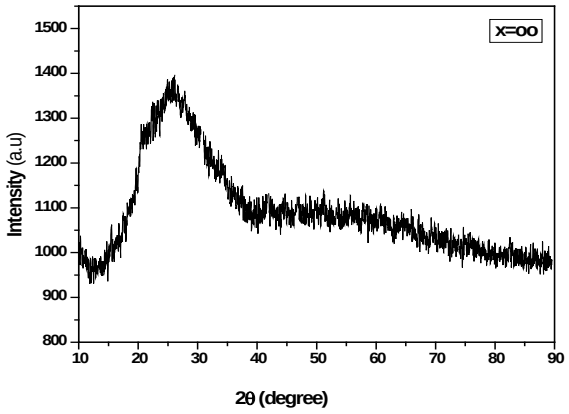

Figure 1(a). XRD pattern for glass system (10-x) SrO -90 V_2O_5

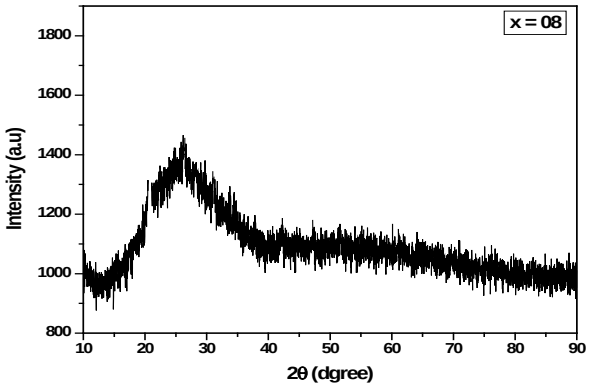

Figure 1(b). XRD pattern for glass system (10-x) SrO -2Fe_2O_3- 90 V_2O_5

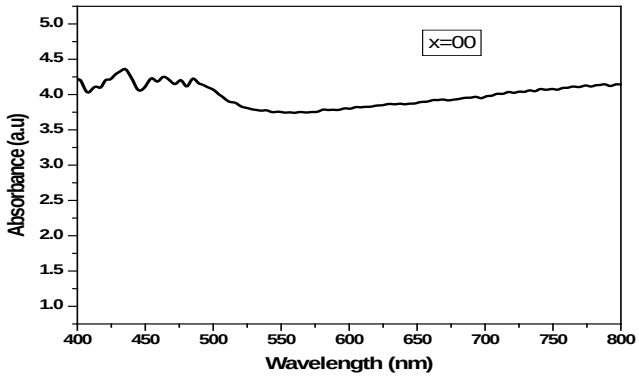

Figure 3(a). Optical absorption as a function of wavelength for the glass system (10SrO-90V_2O_5).

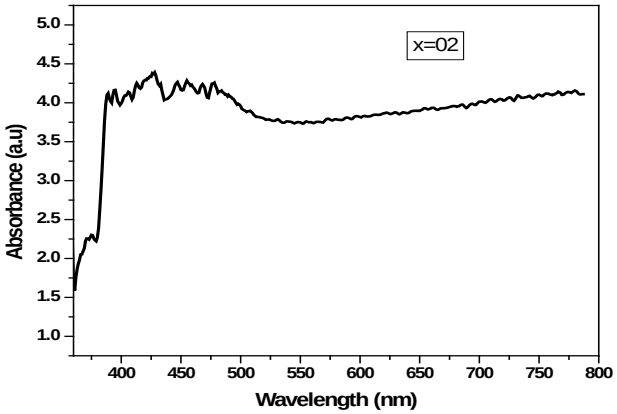

Figure 3(b). Optical absorption as a function of wavelength for the glass system (8SrO-2Fe_2O_3-90V_2O_5)

IJISET - International Journal of Innovative Science, Engineering & Technology, Vol. 3 Issue 7, July 2016
ISSN (Online) 2348 – 7968 | Impact Factor (2015) - 4.332
www.ijiset.com

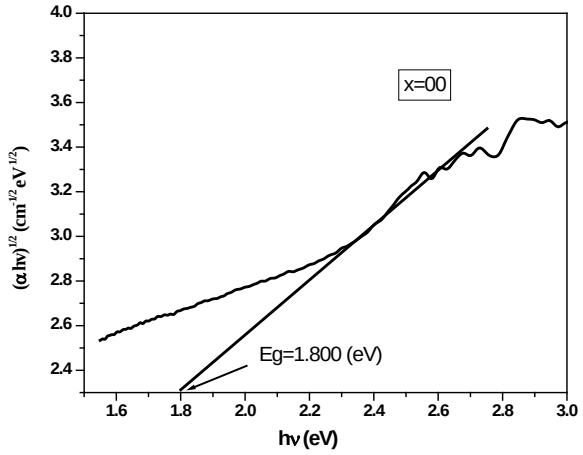

Figure 4(a). Tauc's plots for (10SrO-90V2O5) glass (r =1/2).

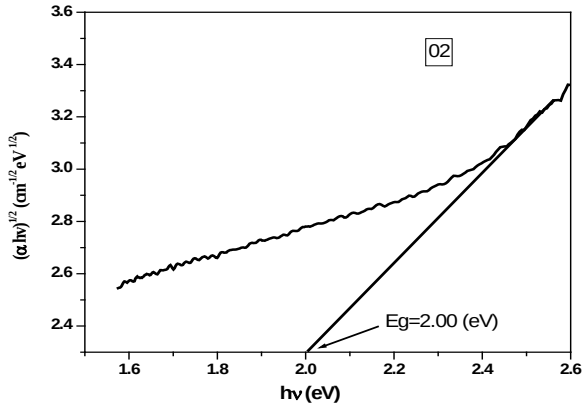

Figure 4(b). Tauc's plots for ($8SrO\text{-}2Fe_2O_3\text{-}90V_2O_5$) glass (r =1/2).

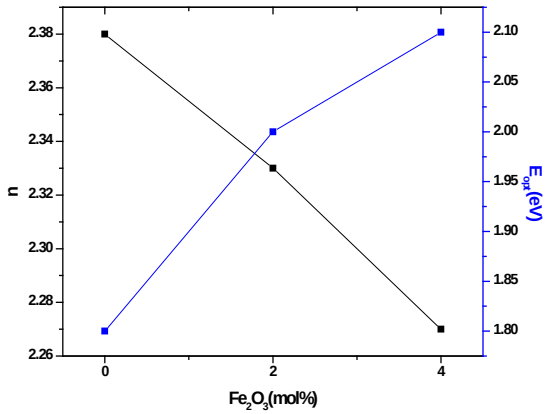

Figure 5. Variation of refractive index (n) and optical energy band gap (E_{opt}) with Fe_2O_3) Content

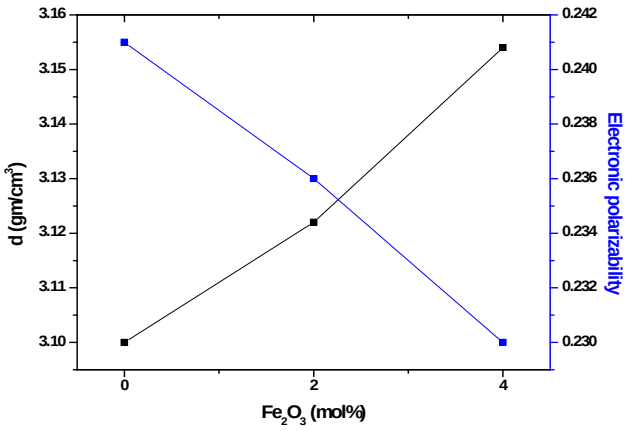

Figure 6 . Variation of density (d) and Electronic polarizability (α_e) with Fe_2O_3 content

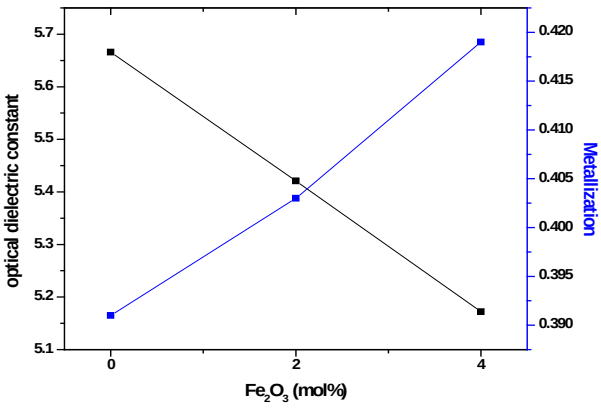

Figure 7 . Variation optical dielectric constant ($\in_p$) and Metallization (M) with Fe_2O_3 content

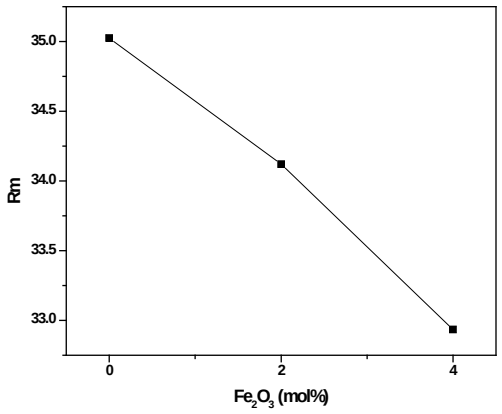

Figure 8. Variation Molar refractivity (Rm) with Fe_2O_3 content

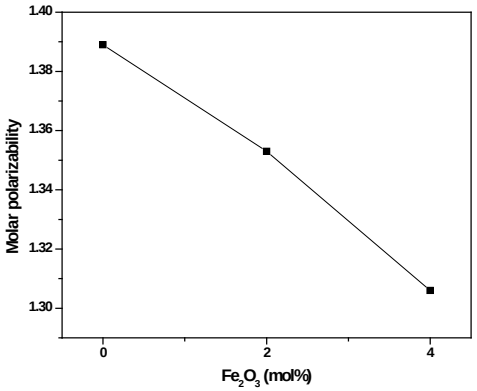

Figure 9. Variation Molar polarizability (α_m) with Fe_2O_3 content

4. Conclusions

The oxide glass samples having a composition (10-x) SrO - x.Fe_2O_3- 90 V_2O_5, where, x = 0, 02, and 04 mole % were successfully prepared by a melt quenching technique. The XRD analysis did not show any sharp peaks and confirmed the amorphous nature of the prepared samples. It has been found that, Fe_2O_3 played an important role in the glass network, by increasing the content of Fe_2O_3. The density and oxygen packing density increases with an increasing the content of Fe_2O_3.

The specific volume and molar volume decreases with an increasing the content of Fe_2O_3. Refractive index reflection loss, molar refractivity, electronic polarizability, molar polarizability, Polarizability per unit volume, decreases with an increasing the content of Fe_2O_3. The optical band gap energy and metallization increases with increasing the content of Fe_2O_3.

References

[1] E. I. Kamitos, Chrysskos, G. D. Patsis, A. P. Karakassides. J. Non-Cryst. Solids 91, (1987)1073.

[2] S. Sen, A. Ghosh, J. Appl. Phys. 86 (1999) 2078.

[3] S. Sen, A. Ghosh, J. Appl. Phys. 87 (2000) 3355.

[4] A. Al-Hajry, A. Al-Shahrani, M.M. El-Desoky , J. Materials Chemistry and Physics 95 (2006) 300.

[5] Sanjay, N. Kishor, A. Agarwal, Indian J.Pure and Appl. Phys. 48, (2010) 205.

[6] Rajesh Parmar, R. S. Kundu, R. Punia, N. Kishore, P. Aghamkar, Journal of Materials,(2013) 5.

[7] Safeya Ibrahim, Mohamed Mahmoud Gomaa, Hussein Darwish, Journal of Advanced Ceramics, 3(2), (2014) 155.

[8] H. A. A. Sidek, M. Hamezan, A.W. Zaidan, Z.A. Talib and K. Kaida Am. J. Applied Sci., 2 (8), (2005) 1266.

[9] Muhammad Altaf , M. Ashraf Chaudhry, J. Mod. Phys.1, (2010) 201.

[10] R. Punia, R. S. Kundu, S. Murugavel and N. Kishore J. Appl. Phys. 112, (2012) 113716.

[11] F. A. Moustafa, M. Abdel-Baki, A. M. Fayad, Fouad El-Diasty,American Journal of Materials Science,4(3),(2014) 119.

[12] Karam Abdel-Aati ALI, Ahmed Gamal El-Din Mostafa, Turk J Phys. 27 (2003), 225.

[13] Muhammad Altaf , M. Ashraf Chaudhry, J. Mod. Phys.1, (2010) 201.

[14] G. Fuxi, Optical and Spectroscopic Properties of Glasses, Springer, Berlin, 1992.

[15] P. Nachimuthu, P. Harikrishnan, R. Jangannatha, Phys. Chem. Glass. 38 (1997), 59.

[16] E.A. Davis, N.F. Mott, Philos. Mag. 22 (1970) 903.

[17] Agarwal, A., V.P. Seth, S. Sanghi, P. Gahlot and S. Khasa, Mater. Lett. 58, (2004) 694.

[18] V. Dimitrov, S. Sakka, J. Appl. Phys. 79 (3) (1996) 1736.

[19] B. Bendow, P.K. Benerjee, M.G. Drexhage, J. Lucas, J. Am. Ceram. Soc 65, (1985) 92.

[20] A. Klinokowski, J. Non-Cryst. Solids 72, (1985), 117.

[21] A. Haralampieva, I. Simeonova-Lozanova, V. Dimitrov, Journal of the University of Chemical Technology and Metallurgy, 47, 4, (2012), 392.

[22] V. Dimitrov, S.Sakka, J. Appl. Phys., 79, (1996), 1741.

[23] D. B. Thombre, M. D. Thombre, International Journal of Engineering Research and Development, 10, 7 (2014), 09.

[24] Asha Rajiv, M. Sudhakara Reddy, Jayagopal Uchil, C. Narayana Reddy, J Adv Sci Res,*5*,2, (2014), *32*.

[25] Dimitrov V, Komatsu T. Journal of Solid State Chemistry, 163, 1, (2002) 100.

[26] Chimalawong P, Kaewkhao J, Kedkaew C, Limsuwan P. J. Physics and Chemistry of Solids, 71, (2010), 965.

[27] Pozza G, Ajo D, Bettinelli M, Speghini A, Casarin M. Solid State Commun, 97, 6, (1996), 521.

[28] Kaminskii, Alexander A, "Laser Crystals - Their Physics and properties", Springer-Verlag, Berlin, (1979). 20.